Determination of Ground- and Excited-State Isomerization Barriers for the Oligothiophene 3',4'-Dibutyl-2,2':5',2''-terthiophene

L. DeWitt,[†] G. J. Blanchard,* E. LeGoff, M. E. Benz, J. H. Liao, and M. G. Kanatzidis

Contribution from the Department of Chemistry and Center for Fundamental Materials Research, Michigan State University, East Lansing, Michigan 48824-1322

Received August 18, 1993[⊛]

Abstract: We report on the crystal structure and rotational isomerization of a poly(alkylthiophene) oligomer, 3',4'-dibutyl-2,2':5',2''-terthiophene. The X-ray crystal structure of this polythiophene oligomer shows an all-*anti* configuration with an ~33° mean dihedral angle between adjacent thiophene rings. Measurements of the torsional barrier to rotation between thiophene rings have been performed for both the ground and first excited singlet states of this oligomer. The S_0 barrier to rotation is measured to be 19.7 kcal/mol using ^{1}H NMR and the S_1 barrier to rotation is determined to be 4.2 kcal/mol using fluorescence lifetime measurements. We discuss the significance of these results in the context of understanding structure/property relationships in poly(alkylthiophenes).

Introduction

Isomerization of labile organic molecules in the solution phase has been studied widely because this conformational variability can affect a range of important physical and chemical properties. Much of this work has been invested in understanding the role isomerization plays in the reaction and photochemistry of labile compounds. Our interest lies in gaining a fundamental understanding of the structure/property relationships for conjugated and nonlinear optical polymers. Of the many possible types of defects present in conjugated polymers, rotational defects are thought to be the most abundant for systems such as polypyrroles and polythiophenes. Rotational defects produce "bends" and "kinks" along the polymer backbone which interrupt and weaken the extent of π-conjugation in a given polymer chain. The extent of conjugation in these polymers determines their utility, and defects along the backbone diminish both their nonlinear optical response and charge carrier mobility. Several classes of conjugated polymers are synthesized in solution, and the incorporation of rotational defects into the polymer is therefore determined, at least in part, by the isomerization barriers exhibited by the constituent oligomers.

Many polymers that contain an extensive conjugated π-electron system become conductive when doped[1] and exhibit large nonlinear optical responses in their undoped form.[2] The field of conducting polymers was initiated with the discovery of conductivity in doped polyacetylene films.[3] Polyacetylene is not an ideal conducting polymer because its conductive response is sensitive to the presence of oxidizing agents and the defect density along individual polymer chains can be controlled to only a limited extent. These material limitations have created interest in more stable conjugated polymers,[4-6] with polythiophenes being one example. While polythiophene is more stable than polyacetylene toward oxidative

degradation, it is also insoluble, limiting its prospects for processability. To make polythiophenes soluble, and therefore processable, 3-alkylthiophenes have been used as monomers.[7-10] This class of polythiophenes not only offers a significant solubility enhancement but also exhibits structural irregularity due to the occurrence of both head-to-head and head-to-tail α-coupling during polymerization. Poly(3-alkylthiophene) can exhibit on the order of 15% of this type of defect.[11] Recently, several ways have been discovered to overcome this intrinsic limit to structural regularity in soluble polythiophenes.[12-16] One approach uses preformed 3',4'-dibutyl-2,2':5',2''-terthiophene (DBTT)[16] as the monomer unit in the synthesis of poly(alkylthiophene).[16] By introducing two alkyl chains on the central thiophene unit, while leaving the terminal thiophene rings without alkyl substituents, the possibility of head-to-head or head-to-tail coupling is obviated, enhancing the regularity of the structure. Nonetheless, there still remains potential ambiguity in the stereochemistry of the oligomer due to rotation about the σ-bonds that connect the individual thiophene rings in DBTT. The purpose of this work is to understand the rotational freedom intrinsic to the oligomer so that we may ultimately know the limits to ordering attainable in the synthesis of poly(DBTT), and, more generally, substituted polythiophenes. We have measured the rotational isomerization barriers for individual DBTT thiophene rings in the ground state using ^{1}H NMR and in the first excited singlet state using fluorescence lifetime measurements. We find that the S_0 barrier to rotation for DBTT is 19.7 kcal/mol, and its S_1 barrier to rotation is 4.2 kcal/mol. In order to understand the dominant confor-

---

* Author to whom correspondence should be addressed.
† Present address: Allied-Signal, Inc., Morristown, NJ 07962.
⊛ Abstract published in *Advance ACS Abstracts*, November 15, 1993.
(1) *Handbook of Conducting Polymers*; Skotheim, T. A., Ed.; Dekker: New York, 1986; Vols. 1 and 2.
(2) Chemla, D. S.; Zyss, J., Eds.; *Nonlinear Optical Properties of Organic Molecules and Crystals*; Academic: 1987; Vol. 2.
(3) Shirikawa, H.; Lewis, E. J.; MacDiarmid, A. G.; Chiang, C. K.; Heeger, A. J. *J. Chem. Soc., Chem. Commun.* 1977, 578.
(4) Chao, S.; Wrighton, M. S. *J. Am. Chem. Soc.* 1987, *109*, 6627.
(5) Mallouk, T. E.; Cammarata, V.; Crayston, J. A.; Wrighton, M. S. *J. Phys. Chem.* 1985, *89*, 5133.
(6) Potember, R. S.; Hoffman, R. C.; Hu, H. S.; Cocchiaro, J. E.; Viands, C. A.; Murphy, R. A.; Poehler, T. O. *Polymer* 1987, *28*, 574.

(7) Jen, K. Y.; Miller, G. G.; Elsenbaumer, R. L. *J. Chem. Soc. Chem. Comm.* 1986, 1346.
(8) Hotta, S.; Rughooputh, S. D. D. V.; Heeger, A. J.; Wudl, F. *Macromolecules* 1987, *20*, 212.
(9) Nowak, M.; Rughooputh, S. D. D. V.; Hotta, S.; Heeger, A. J. *Macromolecules* 1987, *20*, 965.
(10) Sato, M.; Tanaka, S.; Kaeriyama, K. *J. Chem. Soc., Chem. Commun.* 1986, 873.
(11) Zagorska, M.; Krische, B. *Polymer* 1990, *31*, B79.
(12) McCullogh, R. D.; Lowe, R. D. *J. Chem. Soc., Chem. Commun.* 1992, 70.
(13) McCullogh, R. D.; Tristram-Nagle, S.; Williams, S. P.; Lowe, R. D.; Jayaraman, M. *J. Am. Chem. Soc.* 1993, *115*, 4910.
(14) Tour, J. M.; Wu, R. *Macromolecules* 1992, *25*, 1901.
(15) Benz, M. E. Ph.D. Thesis, Michigan State University, East Lansing, MI, 1992.
(16) (a) Wang, C.; Benz, M. E.; LeGoff, E.; Schindler, J. L.; Kannewurf, C. R.; Kanatzidis, M. G. *Polymer Preprints* 1993, *34*, 422. (b) Wang, C.; Benz, M. E.; LeGoff, E.; Schindler, J. L.; Kannewurf, C. R.; Kanatzidis, M. G. Submitted for publication.

mation of DBTT, and thereby establish a structural point of reference for our dynamical measurements, we have performed a detailed X-ray crystal structure examination, and report these results here. Our data show collectively that rotational defects arising from the solution phase polymerization of DBTT occur predominantly at the bonds joining individual terthiophene oligomers and not within the primarily all-*anti* DBTT unit.

Experimental Section

Chemicals. The 3',4'-dibutyl-2,2':5',2''-terthiophene was synthesized and purified according to a published procedure.[15,16] Briefly, tetrabromothiophene was selectively debrominated with *n*-butyllithium to give 3,4-dibromothiophene, which was converted to 3,4-dibutylthiophene by coupling with *n*-butylmagnesium bromide in the presence of a catalyst. Treatment with tetramethylammonium tribromide in a 1:1 mixture of acetic acid and dichloromethane resulted in 2,5-dibromo-3,4-dibutyl-thiophene. Coupling with thiophenemagnesium bromide and a catalyst resulted in the formation of 3',4'-dibutyl-2,2':5',2''-terthiophene. All solvents used for the fluorescence lifetime measurements were purchased from Aldrich Chemical Company as either reagent grade or spectroscopic grade and were used without further purification.

X-ray Diffraction Measurements. Single-crystal X-ray diffraction data for DBTT were collected on a Rigaku AFC6S four-circle diffractometer. Graphite monochromatized Mo Kα radiation was used, and all data were collected at room temperature. Needle-shaped crystals of DBTT were mounted at the ends of glass fibers. The data were collected in the ω scan mode using a scan rate of 8.0°/min (in ω). Each reflection was scanned three times using a scan width of $1.20 + 0.30 \tan \theta°$. The take-off angle was 6°. Accurate cell parameters were determined from 25 machine-centered reflections with $25° < 2\theta < 29°$. The stability of the experimental setup and crystal integrity were monitored by measuring three standard reflections periodically every 150 reflections. No significant crystal decay was observed during data acquisition. The data were corrected for Lorentz–polarization effects and for absorption using ψ scans from three intense reflections with χ near 90° (transmission factors: 0.54–1.12). Anomalous dispersion correction was used for all non-hydrogen atoms. The structure was solved with direct methods (SHELXS-86)[17] and was refined by full-matrix least-squares techniques available in the TEXSAN[18] package of crystallographic programs running on a VAXstation 3100/76 computer. The maximum peak in the final difference electron density map was 0.37 e⁻/Å³. An additional absorption correction according to the DIFABS[19] procedure was applied to isotropically refined data. Equivalent reflections were averaged.

NMR. [1]H spectra of DBTT in perdeuterotoluene were taken on a 300 MHz Gemini VXR NMR spectrometer. The temperature was varied between 20 and 95 °C in these measurements. Uncertainty in the sample temperature was determined to be 0.2 °C.

Steady-State Optical Spectroscopies. The liquid-phase absorption spectrum of DBTT reported here was measured on a Beckman DU-64 spectrophotometer. The resolution of the measurement was ~1 nm over the wavelength range studied. The spontaneous emission spectrum of DBTT was measured using a Perkin-Elmer LS-5 fluorescence spectrophotometer. Data were acquired using 3-nm detection and excitation bandwidths. These data were digitized on a Jandel Scientific digitizing tablet and are shown in Figure 1.

Time Correlated Single Photon Counting Spectrometer. A schematic of the spectrometer used in this work is shown in Figure 2. A CW mode-locked Nd:YAG laser (Quantronix 416) produces ~9 W average power at 1064 nm with 100 ps pulses at 80 MHz. The 1064-nm pulse train is frequency doubled using an angle tuned type II KTP crystal to produce ~900 mW average power at 532 nm. The 532-nm light is used to excite a cavity dumped dye laser (Coherent 702–2). The dye laser is cavity dumped at a repetition rate of 4 MHz and can produce output between 550 and ~1000 nm, depending on the dye and optics used. For these experiments, pulses were generated at 602 nm using Rhodamine 6G (Eastman Kodak), at 650 nm using DCM (Exciton), at 700 nm using LDS-698 (Exciton), and at 750 nm using LDS-751 (Exciton). The output of this laser is between 60 and 150 mW average power depending on the output wavelength, with pulses that exhibit a 5 ps FWHM autocorrelation
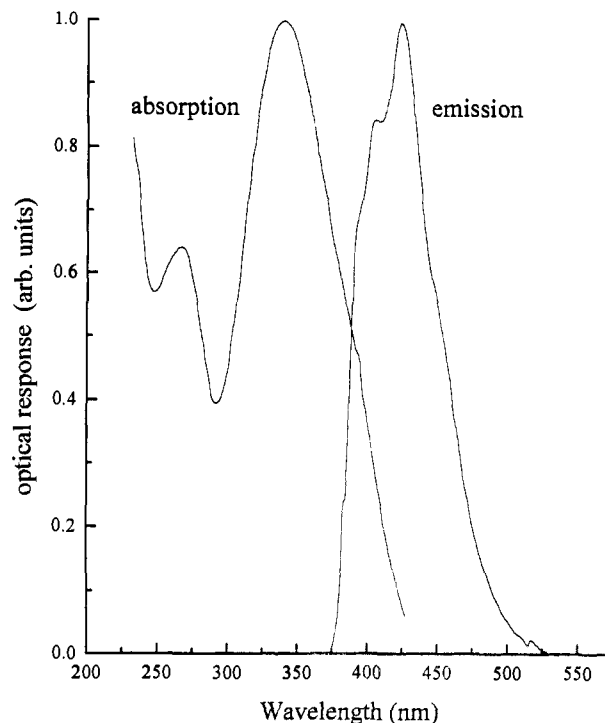
(17) Sheldrick, G. M. In *Crystallographic Computing 3*; Sheldrick, G. M., Kruger, C., Goddard, R., Eds., Oxford University Press: 1985; pp 175–189.

(18) TEXSAN-TEXRAY Structure Analysis Package, *Molecular Structure Corporation*; 1985.

(19) Walker, N.; Stuart, D. *Acta Crystallogr.* **1983**, *A39*, 158.

Figure 1. Absorption and emission spectra of 10⁻⁴ M DBTT in 1-butanol.
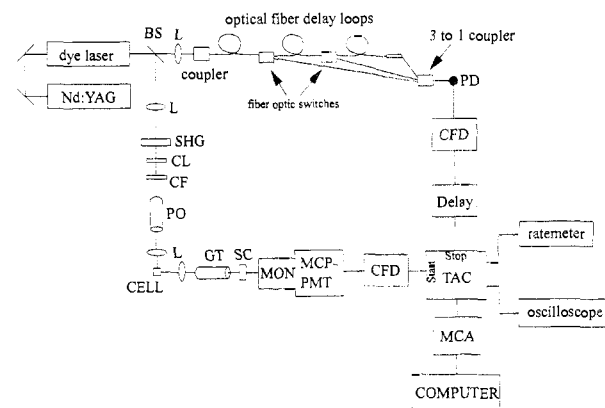

Figure 2. Schematic of the TCSPC spectrophotometer. Abbreviations: BS = beam splitter; FOC = fiber optic coupler; L = focusing lens; SHG = frequency doubling crystal; CL = cylindrical lens; CF = color filter; PO = polarizer; GT = glan-taylor prism, SC = polarization scrambler. Other abbreviations are defined in the text.

trace. The output from the dye laser is divided using a 90/10 beam splitter, with 90% of the light being sent to an angle tuned type I LiIO₃ crystal (2 mm) to produce 301-, 325-, 350-, or 375-nm light. The fundamental is separated from the second harmonic light using color filters and the polarization of the UV pulses is controlled using a fused silica half-wave rhomb (CVI). Typical average UV power at the sample is ≤1 mW. The second harmonic output of the Nd:YAG laser can also be frequency doubled using an angle tuned type I KDP crystal (2 mm) to excite the sample at 266 nm. For all experiments the fluorescence from the sample is collected at 90° with respect to the incident light, and the polarization of the emitted light is selected using a Glan-Taylor prism. The polarization of this selected light is subsequently scrambled, and wavelength selection is carried out using a subtractive double monochromator (American Holographic DB10-S). We use a subtractive double monochromator to eliminate dispersion-induced time broadening of the collected light.[20] The detector, a cooled two stage microchannel plate photomultiplier (MCP-PMT, Hamamatsu R2809U-07), has a rise time of 156 ps and a transit time spread of 42 ps FWHM. The signal from the MCP-PMT is sent directly to one channel of the quad constant fraction discriminator (CFD, Tennelec TC454), where it is processed for input to the time to amplitude converter/biased amplifier (TAC, Tennelec

(20) Holtom, G. R. *Proc. SPIE* **1990**, *1204*, 2.
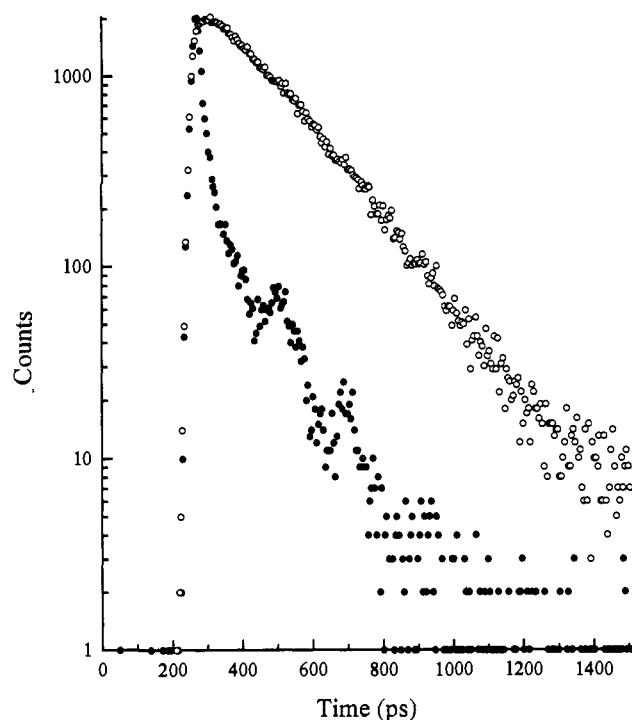
Figure 3. Instrument response function (●) and magic angle lifetime (O) for 10^{-4} M DBTT in 1-octanol.

Table I. Crystal Data and Data Collection and Refinement Parameters for DBTT

empirical formula	$C_{20}H_{24}S_3$
F_{000}	1536
formula weight	360.59
a (Å)	25.094(5)
b (Å)	21.609(5)
c (Å)	7.266(4)
V (Å^3)	3940(4)
space group, Z	$Pbca$ (no. 61), 8
D_{calc}	1.216 g/cm^3
μ (Mo Kα)	3.58 cm^{-1}
crystal dimensions (mm)	0.400 × 0.400 × 1.000
radiation	Mo Kα (λ = 0.710 69 Å)
temp	23 °C
take-off angle	6.0°
$2\theta_{max}$	49.9°
total no. of reflcns measd	3951
structure solution	direct methods
no. observations ($I > 3.00\sigma(I)$)	1497
no. variables	208
reflection/parameter ratio	7.20
residuals: R; R_w[a]	0.081, 0.090
max shift/error in final cycle	0.06

[a] $R = \Sigma\|F_o| - |F_c\|/\Sigma|F_o|$, $R_w = \{\Sigma w(|F_o| - |F_c|)^2/\Sigma w|F_o|^2\}^{1/2}$.

TC864). The system is operated in reverse mode, where the signal channel is input to the TAC start channel. We operate the TAC in reverse mode to avoid electronic dead time limitations which can result in temporal distortions.[21-24] For the reference channel, the remainder of the divided dye laser output ($\sim$10%) is coupled into a 2-m optical fiber and routed to a custom made fiber optic delay line.[25] This delay line consists of fiber optic loops of several different lengths to allow adjustable time offset between the signal and reference channels. This optical delay system allows us to measure fluorescence lifetimes ranging from microseconds to the instrument response function of 25 ps FWHM. The optically delayed laser output is incident on an avalanche photodiode (PD, Hamamatsu S2381), and the signal from the PD is input to a second channel of the quad CFD. The output of the reference CFD channel is delayed electronically (Tennelec TC412A) and sent to the TAC stop channel. TAC output counts are observed using a ratemeter (Tennelec TC525) and a 100-MHz oscilloscope (Tektronix 2230) and are sent to a multichannel analyzer (MCA, Tennelec PCA-II) for collection. The two channels of the quad CFD we use have been modified by the manufacturer for use with MCP-PMT and other fast electrooptic devices. The sample cell (3 mm × 3 mm) we used was made from two adjacent UV grade silica faces and two adjacent blackened silica faces (NSG Precision) to minimize reflections of both the incident radiation and the fluorescence.[20] A typical response function and fluorescence lifetime signal for this system are shown in Figure 3.

Data Analysis. Lifetimes reported are for data deconvoluted from the instrumental response function using software written by Snyder and Demas.[26] The lifetimes we report are averages and standard deviations of at least nine individual determinations for each solvent.

Results and Discussion

It is not uncommon for the excited-state isomerization surface of a molecule to be different than that for its ground state. The

promotion of an electron to an excited state can have a large effect on the equilibrium structure of a molecule.[27-31] Well studied examples of molecules that exhibit state-dependent isomerization surfaces are stilbene[32-40] and the cyanines,[41-44] and this behavior is also known for polymers such as polyphenylene or poly-(phenylenevinylene).[1] In this work we focus on the state-dependent rotational isomerization barrier of DBTT. Our results show that the first excited singlet state barrier to rotation is significantly smaller than the ground-state barrier. Before we discuss these dynamical results in detail, we provide a description of the molecular and crystal structure of DBTT. These structural data provide a point of reference for our torsional barrier measurements.

Ground-State Geometry. The crystallographic data and detailed information on structure solution and refinement for DBTT are listed in Table I. Atomic coordinates and equivalent isotropic thermal parameters of all non-hydrogen atoms are given in Table II, and the structure of DBTT is shown in Figure 4. The two most salient features of the DBTT molecule are that the constituent thiophene rings are in an *anti*-conformation with respect to one another and that the thiophene rings are not coplanar. The two dihedral angles between adjacent thiophene rings are 35.2° and 30.8°, considerably larger than those found in -terthiophene at 6–9°.[45] We view these two dihedral angles in DBTT as essentially the same. Any real difference between these angles reflects the

(21) Nowak, S. A.; Lytle, F. E. *Appl. Spec.* **1991**, *45*, 728.

(22) Nowak, S. A.; Basile, F.; Kivi, J. T.; Lytle, F. E. *Appl. Spec.* **1991**, *45*, 1026.

(23) Seitzinger, N. K.; Hughes, K. D.; Lytle, F. E. *Anal. Chem.* **1989**, *61*, 2611.

(24) Haugen, G. R.; Wallin, B. W.; Lytle, F. E. *Rev. Sci. Instrum.* **1979**, *50*, 64.

(25) Bowman, L. E.; Berglund, K. A.; Nocera, D. G. *Rev. Sci. Instrum.* **1993**, *64*, 338.

(26) Snyder, S.; Demas, J. N. Private communication.

(27) Ben-Amotz, D.; Harris, C. B. *Chem. Phys. Letters* **1985**, *119*, 305.

(28) Shank, C. V.; Ippen, E. P.; Teschke, O.; Eisenthal, K. B. *J. Chem. Phys.* **1977**, *67*, 5547.

(29) Millar, D. P.; Eisenthal, K. B. *J. Chem. Phys.* **1985**, *83*, 5076.

(30) Lacey, A. R.; Craven, F. J. *Chem. Phys. Lett.* **1986**, *126*, 588.

(31) Kang, T. J.; Etheridge, T.; Jarzeba, W.; Barbara, P. F. *J. Phys. Chem.* **1989**, *93*, 1876.

(32) Greene, B. I.; Weisman, R. B.; Hochstrasser, R. M. *J. Chem. Phys.* **1979**, *71*, 544.

(33) Greene, B. I.; Weisman, R. B.; Hochstrasser, R. M. *Chem. Phys.* **1980**, *48*, 289.

(34) Greene, B. I.; Hochstrasser, R. M.; Weisman, R. B. *Chem. Phys. Lett.* **1979**, *62*, 427.

(35) Doany F. E.; Greene, B. I.; Hochstrasser, R. M. *Chem. Phys. Lett.* **1980**, *75*, 206.

(36) Sumitani, M.; Yoshihara, K. *Bull. Chem. Soc. Jpn* **1982**, *55*, 85.

(37) Greene, B. I.; Scott, T. W. *Chem. Phys. Lett.* **1984**, *106*, 399.

(38) Gustafson, T. L.; Roberts, D. M.; Chernoff, D. A. *J. Chem. Phys.* **1983**, *79*, 1559.

(39) Sun, Y. P.; Saltiel, J. *J. Phys. Chem.* **1989**, *93*, 8310.

(40) Park, N. S.; Waldeck, D. H. *Chem. Phys. Lett.* **1990**, *168*, 379.

(41) Rulliere, C. *Chem. Phys. Lett.* **1976**, *43*, 303.

(42) Velsko, S. P.; Waldeck, D. H.; Fleming, G. R. *J. Chem. Phys.* **1983**, *78*, 249.

(43) Iwata, K.; Weaver, W. L.; GustafsonT. L. *J. Phys. Chem.* **1992**, *96*, 10219.

(44) Zhu, X. R.; Harris, J. M. *Chem. Phys.* **1990**, *142*, 301.

(45) Bolhuis, F. V.; Wynberg, H.; Havinga, E. E.; Meijer, E. W.; Staring, E. G. J. *Synth. Met.* **1989**, *30*, 381.
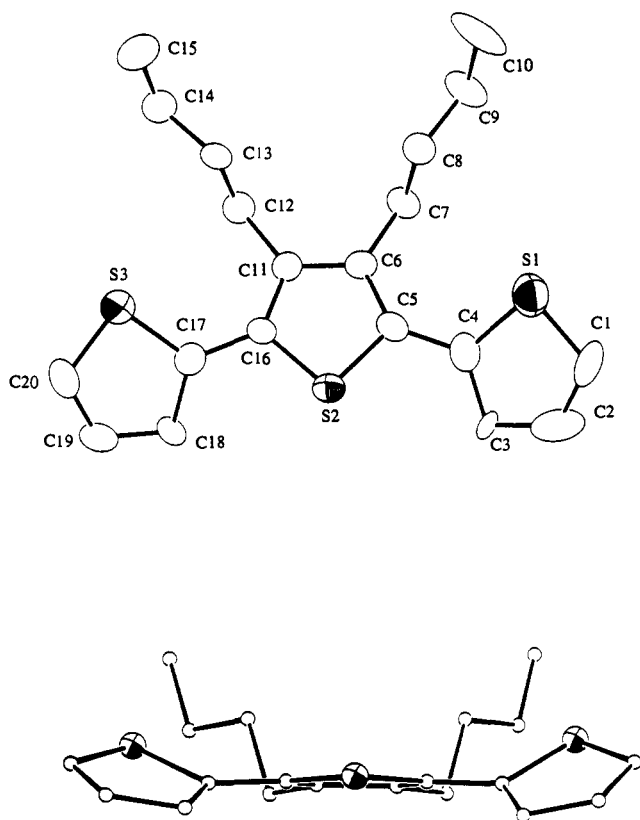
3',4'-Dibutyl-2,2':5',2''-terthiophene

J. Am. Chem. Soc., Vol. 115, No. 25, 1993 12161

Figure 4. Two views of the molecular structure of 3',4'-dibutyl-2,2': 5',2''-terthiophene, DBTT, with labeling scheme. In the bottom view, the temperature factors of the carbon atoms were set artificially small for clarity.

flatness of the torsional potential surfaces for thiophene ring rotation where the angles between adjacent rings are substantially different from 90°. Absent any anomalous packing forces, the significant difference in geometry between DBTT and α-ter-thiophene must be due to the presence of the n-butyl groups. The two n-butyl side chains of the central ring are fully extended, adopting a *trans* conformation to minimize steric crowding. These findings suggest that similar differences exist between poly(3-alkylthiophene) or poly(DBTT) and polythiophene. The isotropic equivalent temperature factors of the sulfur atoms in the terminal thiophene ring are roughly twice that of the central sulfur atom (see Table II) indicating enhanced mobility around C–C bridging σ-bonds. Selected bond distances and angles are given in Table III. The longest C–C bonds in the terthiophene backbone are those joining the thiophene rings at 1.47(1) and 1.46(1) Å, respectively. These values are essentially the same as those reported for α-terthiophene. However, these values are significantly shorter than the length of a pure single C–C bond indicating considerable double bond character and π-delocalization across the three rings of DBTT, despite the relatively large ($\sim$33°) dihedral angles between adjacent thiophene rings.

Ground-State Barrier Measurement. ^{1}H NMR spectra of DBTT were obtained using a 300-MHz spectrometer. At a sample temperature of 25 °C, DBTT in perdeuterotoluene produced the spectrum shown in Figure 5a. The splitting and shifting of the peaks corresponding to the aromatic protons located between 6.8 and 7.2 ppm (inset to Figure 5a) was observed to depend on the sample temperature. Between 85 °C and 90 °C we are able to distinguish the coalescence of two distinct chemical environments for the aromatic protons on the outer thiophene rings (Figure 5b,c). The temperature-dependent shifts seen for the resonances at δ ~7.05 ppm are for the 4 and 3'' protons. These data show that, in addition to splitting, the local environments of these protons change in an absolute sense with temperature. We believe this

Table II. Positional Parameters and Equivalent Isotropic Displacement Values (Å^2)^a for DBTT with Estimated Standard Deviations in Parentheses

atom	x	y	z	B(eq)
S1	0.5658(2)	–0.1509(2)	0.2787(5)	8.3(2)
S2	0.6747(1)	–0.0081(1)	0.1394(3)	4.7(1)
S3	0.7051(1)	0.1747(1)	0.3425(5)	7.0(2)
C1	0.5774(5)	–0.2093(5)	0.127(2)	7.1(7)
C2	0.6237(5)	–0.2015(6)	0.036(2)	7.7(7)
C3	0.6541(3)	–0.1498(4)	0.073(1)	3.0(4)
C4	0.6252(4)	–0.1163(4)	0.215(1)	4.8(5)
C5	0.6404(3)	–0.0558(4)	0.291(1)	4.0(4)
C6	0.6365(4)	–0.0284(4)	0.462(1)	4.1(5)
C7	0.6096(3)	–0.0602(5)	0.621(1)	4.6(5)
C8	0.5513(4)	–0.0452(5)	0.645(1)	5.0(5)
C9	0.5233(4)	–0.0806(6)	0.798(2)	7.2(7)
C10	0.4675(5)	–0.0647(8)	0.825(2)	11(1)
C11	0.6602(3)	0.0308(4)	0.471(1)	3.9(4)
C12	0.6649(4)	0.0698(5)	0.644(1)	5.3(5)
C13	0.6185(4)	0.1153(5)	0.668(1)	5.2(5)
C14	0.6291(5)	0.1605(6)	0.826(2)	7.6(7)
C15	0.5838(6)	0.2037(6)	0.858(2)	9.5(9)
C16	0.6840(3)	0.0477(4)	0.306(1)	4.1(4)
C17	0.7151(4)	0.1019(4)	0.252(1)	4.5(5)
C18	0.7534(3)	0.1038(4)	0.111(1)	4.2(4)
C19	0.7721(4)	0.1645(5)	0.090(2)	6.2(6)
C20	0.7510(4)	0.2062(5)	0.199(2)	6.1(6)
H1	0.5531	–0.2465	0.1123	7.5
H2	0.6348	–0.2334	–0.0546	7.8
H3	0.6862	–0.1381	0.0145	3.1
H4	0.6128	–0.1047	0.6052	5.3
H5	0.6281	–0.0499	0.7327	5.3
H6	0.5477	–0.0013	0.6704	5.8
H7	0.5328	–0.0526	0.5302	5.8
H8	0.5273	–0.1247	0.7682	7.9
H9	0.5435	–0.0742	0.9092	7.9
H10	0.4632	–0.0217	0.8537	10.3
H11	0.4470	–0.0720	0.7119	10.3
H12	0.4508	–0.0885	0.9192	10.3
H13	0.6658	0.0436	0.7519	6.5
H14	0.6973	0.0932	0.6426	6.5
H15	0.6140	0.1374	0.5527	6.2
H16	0.5862	0.0922	0.6878	6.2
H17	0.6357	0.1364	0.9380	8.4
H18	0.6623	0.1824	0.8022	8.4
H19	0.5901	0.2325	0.9514	9.6
H20	0.5780	0.2279	0.7424	9.6
H21	0.5516	0.1820	0.8788	9.6
H22	0.7660	0.0680	0.0378	4.6
H23	0.7992	0.1762	–0.0037	7.2
H24	0.7609	0.2512	0.1979	7.4

^{a} $B(\text{eq}) = \frac{4}{3}[a^2\beta_{11} + b^2\beta_{22} + c^2\beta_{33} + ab(\cos\gamma)\beta_{12} + ac(\cos\beta)\beta_{13} + bc(\cos\alpha)\beta_{23}]$.

is because of temperature-dependent changes in the motional freedom of the n-butyl groups at the 3' and 4' positions. The different environments responsible for the splitting of these proton resonances arise from different rotameric forms of the oligomer. The splitting seen for the 4 and 3'' protons and for the 2 and 5'' protons (δ ~6.87 ppm) coalesce at the same temperature. From these line widths and the observed coalescence temperature we can calculate the ground-state barrier to ring rotation in DBTT[46]

$$\Delta G^{\text{isom}} = 4.575 \times 10^{-3} T_c \left[9.972 + \log_{10}\left(\frac{T_c}{\delta\nu}\right) \right]$$

where T_c is the coalescence temperature, $\delta\nu = 4.65$ Hz is the full width at half maximum of the coalesced resonance at T_c, and the units of ΔG^{isom} are kcal/mol. From our data we find $\Delta G^{\text{isom}} = 19.7 \pm 0.3$ kcal/mol for S_0 DBTT. While this is a large torsional barrier, it is not inconsistent with that of other organic molecules, such as *trans* stilbene[32–37] and 3,3'-diethyloxadicarbocyanine iodide (DODCI)[41] which exhibit isomerization about their polyene bonds, or several other molecules where the isomerization involves

(46) Sandstrom, J. *Dynamic NMR Spectroscopy*; Academic Press: New York, 1982; pp 78–121.

Table III. Selected Bond Distances (Å) and Angles (deg) for DBTT with Standard Deviations in Parentheses[a]

bond	distance (Å)	bond	distance (Å)
C1–S1	1.70(1)	C7–C8	1.51(1)
S1–C4	1.73(1)	C8–C9	1.52(1)
S2–C5	1.735(9)	C9–C10	1.46(1)
S2–C16	1.724(9)	C11–C12	1.52(1)
S3–C17	1.72(1)	C11–C16	1.39(1)
S3–C20	1.70(1)	C12–C13	1.53(1)
C1–C2	1.35(2)	C13–C14	1.53(1)
C2–C3	1.38(2)	C14–C15	1.49(2)
C3–C4	1.45(1)	C16–C17	1.46(1)
C4–C5	1.47(1)	C17–C18	1.41(1)
C5–C6	1.38(1)	C18–C19	1.40(1)
C6–C7	1.50(1)	C19–C20	1.31(1)
C6–C11	1.41(1)		

atoms	angle (deg)	atoms	angle (deg)
C1–S1–C4	90.0(6)	C8–C9–C10	115(1)
C5–S2–C16	92.2(5)	C6–C11–C12	124.6(9)
C17–S3–C20	91.9(5)	C6–C11–C16	112.5(8)
S1–C1–C2	111.9(9)	C12–C11–C16	122.5(8)
C1–C2–C3	119(1)	C11–C12–C13	113.0(9)
C2–C3–C4	105.7(8)	C12–C13–C14	111.2(9)
S1–C4–C3	113.7(7)	C13–C14–C15	112(1)
S1–C4–C5	120.7(8)	S2–C16–C11	111.3(7)
C3–C4–C5	125.4(8)	S2–C16–C17	116.4(7)
S2–C5–C4	115.0(7)	C11–C16–C17	132.2(9)
S2–C5–C6	110.6(7)	S3–C17–C16	123.5(7)
C4–C5–C6	134.3(9)	S3–C17–C18	125.6(8)
C5–C6–C7	121.9(9)	C16–C17–C18	125.6(8)
C5–C6–C11	113.3(8)	C17–C18–C19	109.5(9)
C7–C6–C11	124.8(9)	C18–C19–C20	116(1)
C6–C7–C8	115.2(8)	S3–C20–C19	111.7(8)
C7–C8–C9	115.0(8)		

[a] Mean bond lengths are calculated from $l = (\sum_n l_n)/n$. The estimated standard deviations in the mean bond lengths are calculated from $\sigma = [(\sum_n (l_n - l)^2)/(n - 1)]^{1/2}$ where l_n is the length of the nth bond, l is the mean length, and n is the number of measurements of the same bond.

rotation of adjacent ring structures.[47–50] Other experimental data from which the isomerization barrier of different thiophene oligomers can be inferred are also consistent with our measurement.[51–54]

Reorientation Times. It is important to consider any possible conformer-specific solvation effects on DBTT because such an effect could alter the distribution of structures in solution and thus have an effect on the measured torsional barriers. In addition, semiempirical AM1 calculations indicate that both the optical and dipolar properties of the three conformers shown in Figure 6 are different enough that the reorientation dynamics of II may be discernible from those of I and III. The change in dipole moment upon excitation predicted for II suggests that we should consider excited-state complexation to the solvent,[55–60] while the same is not true for I or III. In addition, the S_0–S_1 origin of II is predicted to be blue shifted by ~250 meV from the origins for I and III, indicating the contribution of multiple rotamers to the absorption and emission profiles measured for DBTT (Figure 1).

(47) Leete, E.; Riddle, R. M. *Tetrahedron Lett.* **1978**, *52*, 5163.
(48) Kashima, C.; Maruyama, T.; Fujioka, Y.; Harada. K. *J. Phys. Org. Chem.* **1988**, *1*, 185.
(49) Nishida, A.; Akagawa, Y.; Shirakawa, S.; Fujisaki, S.; Kajigaeshi, S. *Can. J. Chem.* **1991**, *69*, 615.
(50) Mitchell, R. H.; Shue-Hen Yan, J. *Can. J. Chem.* **1980**, *58*, 2584.
(51) dos Santos, D. A.; Galvao. D. S.; Laks, B.; dos Santos, M. C. *Chem. Phys. Lett.* **1991**, *184*, 579.
(52) Faid, K.; Leclerc, M. *J. Chem. Soc.. Chem. Commun.* **1993**, 962.
(53) Barbarella, G.; Zambianchi, M.; Bongini, A.; Antolini, L. *Adv. Mater.* **1992**, *4*, 282.
(54) Kawase, T.; Ueno, N.; Oda, M. *Tetrahedron Lett.* **1992**, *33*, 5405.
(55) Blanchard, G. J. *Chem. Phys.* **1989**, *138*, 365.
(56) Blanchard, G. J. *J. Phys. Chem.* **1991**, *95*, 5293.
(57) Blanchard, G. J. *Anal. Chem.* **1989**, *61*, 2394.
(58) Blanchard, G. J. *J. Phys. Chem.* **1989**, *93*, 4315.
(59) Blanchard, G. J. *J. Phys. Chem.* **1988**, *92*, 6303.
(60) Blanchard, G. J.; Cihal, C. A. *J. Phys. Chem.* **1988**, *92*, 5950.

It is important to establish the presence or absence of conformation-dependent dynamics in DBTT to address the role that site-specific solvation effects play in determining its isomerization barriers. We investigated this possibility by measuring the excitation and emission wavelength dependence of the orientational relaxation time of DBTT in 1-butanol. We excited DBTT at 301, 325, 350, and 375 nm and collected fluorescence decays for polarizations parallel and perpendicular to the excitation polarization at 410, 435, and 454 nm. Reorientation times for DBTT were measured for all combinations of the four excitation wavelengths with the three emission wavelengths. We observed no dependence of reorientation time on either the excitation or emission wavelength, to within our experimental uncertainty. For DBTT in 1-butanol, $\tau_{or} = 128 \pm 13$ ps. If there is any conformation-dependence in the interaction between DBTT and the surrounding medium, it will be too weak to affect the isomerization of the oligomer measurably.

Excited-State Barrier Measurement. Dilute (~10^{-4} M) solutions of DBTT in normal alcohols methanol through 1-octanol and 1-decanol were excited at 301 nm and fluorescence was collected at 410, 435, and 454 nm to ensure the contribution of only one excited electronic state to our data. The lifetimes were observed by collecting at the magic angle (54.7°) to eliminate rotational diffusion contributions to the data. The fluorescence lifetime of the oligomer depends linearly on the solvent viscosity (see Figure 7). We can understand this behavior as follows. The most efficient relaxation pathway, which determines the excited state lifetime, is accessible to all of the conformers through rotation about the σ-bonds. One possibility is that the 90° conformer (adjacent rings perpendicular) exhibits efficient relaxation to the ground state surface, as is seen for stilbene,[32–37] although the S_1 isomerization surfaces of stilbene and DBTT likely differ substantially. Another possibility is that one of the conformers is coupled more strongly to the ground state than the others, and the lifetime of the excited state is mediated by the time it takes the molecule to isomerize to that particular conformation. Regardless of the exact identity of the dominant relaxation pathway, as the individual thiophene rings rotate, they encounter two distinct barriers to rotation, one intrinsic to the molecule and one imposed by the solvent cage. The portion of the barrier contributed by the solvent can be controlled by varying the solvent viscosity. As the viscosity is increased, the measured excited-state lifetimes increase due to the larger effective barrier to thiophene ring rotation. The lifetimes we measure for DBTT range from 124 ± 3 ps in methanol to 177 ± 11 ps in 1-decanol (Table IV). These data on DBTT are consistent with work on stilbene showing that the rate of *cis–trans* isomerization is decreased with increasing solvent viscosity.[61,62] Extrapolation of the lifetime dependence on viscosity to zero viscosity yields the intramolecular barrier to rotation. Regression of our data shows a zero viscosity lifetime of 123 ± 2 ps.

$$k_{isom} \cong \frac{1}{\tau_{fl}^{\eta=0}} = A \exp(-\Delta E / RT)$$

For $A = 10^{13}$ (appropriate for the alcohols), $\Delta E = 4.2$ kcal/mol. The uncertainty in this barrier height is ultimately determined by our knowledge of A. We estimate an uncertainty of ±0.4 kcal/mol based on an uncertainty of a factor of 2 in A. This result is also consistent with measurements on cyanines, where an excited-state isomerization barrier of 3–5 kcal/mol is observed.[41]

Our data also provide insight into internal conversion in DBTT. Exciting DBTT in 1-butanol at 266 nm yields a lifetime of 148 ± 2 ps, significantly longer than the same solution excited at 350 nm ($\tau_{fl} = 136 \pm 2$ ps). The ~12 ps difference is the time required

(61) Courtney, S. H.; Fleming, G. R. *J. Chem. Phys.* **1985**, *83*, 215.
(62) Rothenberger, G.; Negus, D. K.; Hochstrasser, R. M. *J. Chem. Phys.* **1983**, *79*, 5360.
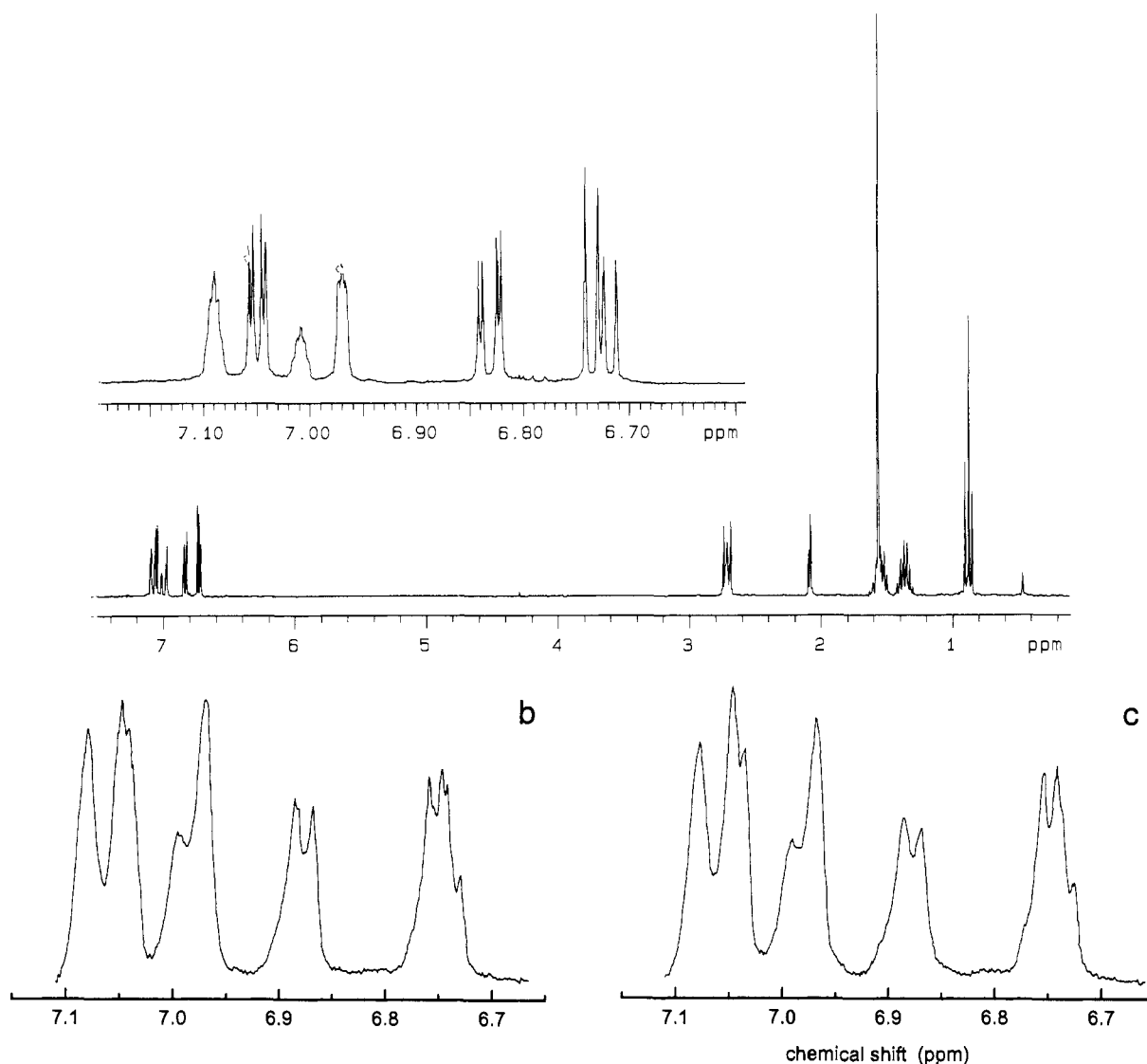
Figure 5. (a) ¹H NMR spectrum of DBTT in perdeuterotoluene at 25 °C. The inset shows an expanded view of the aromatic proton region. Splitting of the aromatic protons between 85 °C (b) and 90 °C (c) shows that the ground-state barrier to rotation lies in this temperature range.
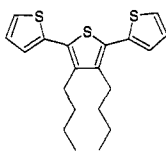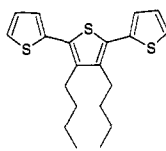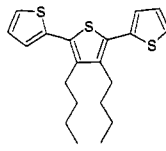

Figure 6. AM1 calculated results for transition energies and change in dipole moment for three rotameric forms of DBTT.

for the excitation to relax to the S_1 surface from the higher excited state, presumably S_2.

Comparison to Literature Data on Thiophene Oligomers. There have been several other reports in the recent literature that provide information relevant to estimating the ground-state torsional barrier for thiophene oligomers. A recent AM1 computational study on alkylthiophene short oligomers has indicated a ground-state torsional barrier of ~3 kcal/mol for a sterically strained (head-to-head) dialkylbithiophene, with lower barriers for the less hindered (head-to-tail and tail-to-tail) coupled ring systems.[51] We have calculated this barrier for DBTT using the AM1 Hamiltonian with configuration interaction, and our results indicate a similar ground state torsional barrier of ~3.7 kcal/mol for DBTT. One possible explanation for the consistently low ground-state torsional energies predicted by the AM1 methods is that the bonds joining the thiophene rings are predicted to have a bond order lower than that observed experimentally. Resonance contributions to the inter-ring bonds that increase their bond order would serve to make the system more resistant to torsional motions, but such a resonance structure would involve the formation of a biradical. It is also possible that the spatial extent of the sulfur orbitals is not modeled well by the AM1 parameterization. Regardless of the reasons for the difference between calculated and experimental results, we can conclude that AM1 calculations do not model thiophene oligomer torsional barriers well.

Experimental information on the conformation and motional freedom of thiophene rings in oligomeric polythiophenes suggests
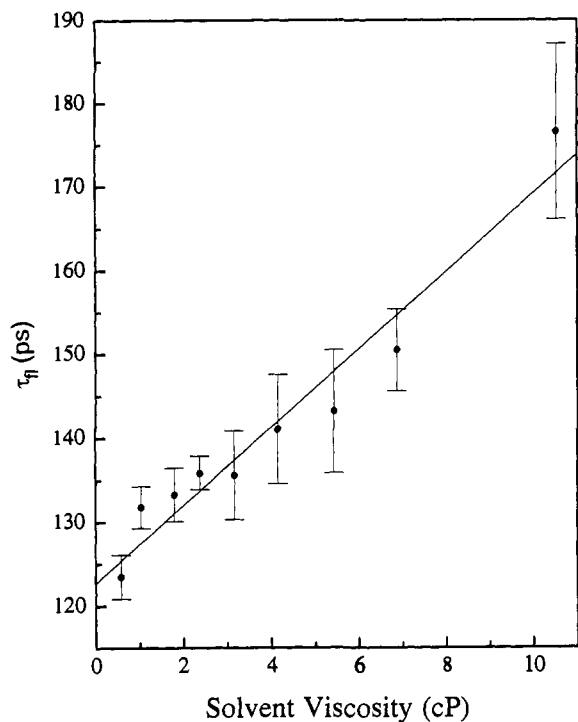
Figure 7. Dependence of DBTT fluorescence lifetimes on the solvent viscosity.

Table IV. Fluorescence Lifetime Data for DBTT in Primary *n*-Alcohols[a]

solvent	viscosity (cP)	τ_{fl} (ps)
methanol	0.576	124 ± 3
ethanol	1.032	132 ± 3
1-propanol	1.796	133 ± 3
1-butanol	2.377	136 ± 2
1-pentanol	3.160	136 ± 6
1-hexanol	4.146	141 ± 7
1-heptanol	5.427	143 ± 7
1-octanol	6.878	151 ± 5
1-decanol	10.524	177 ± 11

[a] The reported uncertainties are standard deviations for a minimum of nine determinations in each solvent.

that the individual thiophene rings of the oligomer are rotated at ~40° with respect to one another in chloroform solution, although direct experimental evidence for this assertion is not provided.[53] The steric interactions between the thiophene sulfur and the *n*-butyl tails of DBTT yield an equivalent result. The lowest energy crystalline conformation of DBTT is all-*anti* with the terminal thiophene rings rotated ~33° with respect to the center 3,4-dibutylthiophene ring. The temperature-dependence of the linear optical response of di-*n*-hexylterthiophene (DHTT) oligomers has also been reported recently.[52] No direct attempt was made to extract the torsional barrier energy from these data, although the authors note that at the melting point of the hexamer, bi(DHTT), there is no abrupt change in the absorption maximum.

This finding suggests that the bi(DHTT) oligomer largely retains its solid-state conformation until 46° above the melting point, where the onset of a blue shift in the absorption maximum is noted. Thus, even for larger oligomers with labile substituents, there is a substantial barrier to torsional motion.

Conclusions

We have determined a 19.7 kcal/mol isomerization barrier in the ground state and a 4.2 kcal/mol barrier to rotation in the first excited singlet state of DBTT. These results demonstrate that the DBTT oligomer can circumvent many of the defects associated with using the alkylthiophenes for polymerization, but there necessarily still remains some structural irregularity in poly-(DBTT) resulting from a distribution of orientations about the bridging σ-bonds between oligomers. This degree of disorder for poly(DBTT) is comparatively small, but not insignificant, as even low defect densities in π-conjugation can diminish the conductive and nonlinear optical properties of the polymer. Synthesis of more highly ordered precursors will be required to increase the conductivity of doped polythiophene films and to optimize the nonlinear optical response of undoped forms. In addition to enhanced structural regularity, such an oligomer would require a rotationally asymmetric polymerization condition to avoid statistical disorder over a longer length scale.[13] The use of longer oligomers for the synthesis of polythiophenes may not prove useful because of the apparently lower barriers to intramolecular rotation exhibited by these compounds.[52,63] The judicious design and optimization of substituted bithiophene and terthiophene oligomers[64] appears to offer the best route to the most highly ordered poly(alkylthiophenes).

Supplementary Material Available: Tables of the structure determination, atom coordinates, bond distances, bond angles, anisotropic thermal parameters, and torsion angles for DBTT (7 pages); tables of observed and calculated structure factors (24 pages). This material is contained in many libraries on microfiche, immediately follows this article in the microfilm version of the journal, and can be ordered from the ACS; see any current masthead page for ordering information.

(63) Kanatzidis, M. G.; Liao, J. H.; Benz, M. E.; LeGoff, E. Submitted for publication.

(64) Larger oligomers are undesirable because oxidation yields stable radical cations which polymerize slowly and lead to low molecular weight materials.